Optics & Laser Technology 57 (2014) 129–135

Contents lists available at ScienceDirect

Optics & Laser Technology

journal homepage: www.elsevier.com/locate/optlastec

Dynamic visual cryptography for optical assessment of chaotic oscillations

Vilma Petrauskiene [a], Arvydas Survila [b], Algimantas Fedaravicius [c], Minvydas Ragulskis [a,*]

[a] Research Group for Mathematical and Numerical Analysis of Dynamical Systems, Kaunas University of Technology, Studentu 50-222, Kaunas LT-51368, Lithuania
[b] Institute of Defense Technology, Kaunas University of Technology, Lithuania
[c] Institute of Defense Technology, Kaunas University of Technology, Lithuania

ARTICLE INFO

Article history:
Received 26 July 2013
Received in revised form
16 September 2013
Accepted 12 October 2013

Keywords:
Visual cryptography
Chaotic oscillations
Time average moiré

ABSTRACT

An optical experimental technique based on dynamic visual cryptography is proposed for the optical assessment of chaotic oscillations. The secret image is embedded into a single cover image which is fixed onto the surface of the oscillating structure. It is demonstrated that this visual scheme is applicable for the assessment of chaotic oscillations even though time-averaged moiré fringes do not form when the encoded cover image is oscillated by the chaotic law. The decoding process is completely visual – a simple visual inspection can be used to determine if the parameters of the chaotic oscillations are kept in the tolerated range.

1. Introduction

Visual cryptography is a cryptographic technique which allows visual information to be encrypted in such a way that the decryption can be performed by the human visual system, without the aid of computers. Visual cryptography was pioneered by Naor and Shamir in 1994 [1]. They demonstrated a visual secret sharing scheme, where the secret image was broken up into n shares so that only someone with all n shares could decrypt the image, while any $n-1$ shares revealed no information about the original image. Many advances in visual cryptography have been done since 1994. Visual cryptography for color images has been proposed in [2,3]. Ideal contrast visual cryptography schemes have been introduced in [4]. A general multi-secret visual cryptography scheme is presented in [5]; incrementing visual cryptography is described in [6]. A new cheating prevention visual cryptography scheme is discussed in [7]. The concept of dynamic visual cryptography was introduced in [8]. This method is based not on static superposition of shares, but on time-average geometric moiré applied for a single encoded image. This method generates only one cover image and the secret image can be interpreted by the naked eye only when the encoded cover image is harmonically oscillated in a predefined direction at pre-set amplitude of oscillation. Additional image security measures are implemented in [9,10], where the secret image is leaked in a form of a pattern of time-averaged moiré fringes only when the encrypted cover image is oscillated according to a predefined law of motion.

Visual cryptography has been used in a number of important information security applications. In particular, dynamic visual cryptography has been successfully exploited for optical control of harmonically vibrating systems and vibration generation equipment [11]. But it is well known that a periodic force applied to a nonlinear system can cause a chaotic response. The damped and harmonically driven nonlinear pendulum is a paradigmatic model exhibiting such phenomena as frequency-locking and chaos [12]. In general, such complex chaotic responses can be observed in many different systems – including biological, chemical and, of course, technical systems [13,14]. A computational framework for digital implementation of dynamic visual cryptography based on chaotic oscillations is presented in [15]. But an effective experimental implementation of a chaotic visual cryptography remains an open question.

Thus, the main objective of this paper is to investigate the feasibility of chaotic dynamic visual cryptography where the time function determining the deflection of the encoded image from the state of equilibrium is a Gaussian process with zero mean and pre-determined variance.

This paper is organized as follows. The optical background and main relationships are discussed in Section 2; the encoding scheme used for dynamic visual cryptography is described in

* Corresponding author. Tel.: +370 69822456; fax: +370 37330446.
E-mail addresses: vilma.petrauskiene@ktu.lt (V. Petrauskiene), arvydas.survila@ktu.lt (A. Survila), algimantas.fedaravicius@ktu.lt (A. Fedaravicius), minvydas.ragulskis@ktu.lt (M. Ragulskis).
URL: http://www.personalas.ktu.lt/~mragul (M. Ragulskis).

0030-3992/$ - see front matter © 2013 Elsevier Ltd. All rights reserved.
http://dx.doi.org/10.1016/j.optlastec.2013.10.015

Section 3; results of computational experiments are presented in Section 4; the experimental implementation of dynamic visual cryptography is described in Section 5; experimental results are discussed in Section 6; concluding remarks and the discussion on other potential applications of the presented technique are given in the concluding section.

2. Optical background

One-dimensional harmonic moiré grating reads

$$F(x)=\frac{1}{2}+\frac{1}{2}\ \sin\left(\frac{2\pi}{\lambda}x\right) \tag{1}$$

where x is the longitudinal coordinate; λ is the pitch of the moiré grating; 1 corresponds to white color; 0 corresponds to black color and all intermediate values correspond to an appropriate grayscale level.

Time-average geometric moiré is an optical experimental method when the moiré grating is formed on the surface of an oscillating structure and time averaging techniques are used for the registration of time averaged patterns of fringes [16]. Let $\xi(t)$ is a function describing dynamic deflection from the state of equilibrium ($\xi=0$ corresponds to the state of equilibrium; t is time). Then, time-averaged image of the moiré grating reads

$$\overline{F}(x)=\lim_{T\to\infty}\frac{1}{T}\int_0^T F(x-\xi(t))dt \tag{2}$$

where T is the exposure time.

A periodic moiré grating can be expanded into the Fourier series

$$F(x)=\frac{a_0}{2}+\sum_{k=1}^{+\infty}\left(a_k\ \cos\left(\frac{2\pi k}{\lambda}x\right)+b_k\ \sin\left(\frac{2\pi k}{\lambda}x\right)\right) \tag{3}$$

where λ is the pitch of the grating. Let us denote $p_\xi(x)$ as the density function of the time function $\xi(t)$. In other words, $p_\xi(x)$ describes the statistical distribution of the deflection from the state of equilibrium. It is shown in [9] that if $p_\xi(x)$ is a symmetric function, then the time averaged image of the moiré grating oscillated according to the time function $\xi(t)$ (as the exposure time T tends to infinity) reads:

$$\overline{F}(x)=\frac{a_0}{2}+\sum_{k=1}^{+\infty}\left(a_k\ \cos\left(\frac{2\pi k}{\lambda}x\right)+b_k\ \sin\left(\frac{2\pi k}{\lambda}x\right)\right)P_\xi\left(\frac{2\pi k}{\lambda}\right) \tag{4}$$

where P_ξ is the Fourier transform of $p_\xi(x)$. In other words, the time averaged image is blurred according to the function $p_\xi(x)$ – it is a convolution of the static moiré grating and the uni-directional point spread function defining the motion around the state of equilibrium. It is shown in [15] that the Fourier transform of the Gaussian density function representing stochastic oscillations around the state of equilibrium reads

$$P_\xi\left(\frac{2\pi k}{\lambda}\right)=\exp\left(-\frac{1}{2}\left(\frac{2\pi k\sigma}{\lambda}\right)\right) \tag{5}$$

where σ is the standard deviation of the Gaussian process.

A harmonic moiré grating comprises an array of parallel lines. Then, the coefficients of the Fourier expansion read (Eq. (1)): $a_0=1$; $a_1=0.5$; $a_{2,3,\ldots}=0$ $b_{1,2,\ldots}=0$. Thus the envelope function characterizing the decay of the contrast of the time-averaged moiré grating blurred by chaotic oscillations reads [15]

$$\overline{E}(\sigma)=\frac{1}{2}\pm\frac{1}{2}\exp\left(-\frac{1}{2}\left(\frac{2\pi\sigma}{\lambda}\right)\right) \tag{6}$$

note that no time-averaged fringes are formed by chaotic oscillations – the moiré grating is monotonically blurred as the standard deviation σ is increased (Fig. 1). Really, the sharp image of the static harmonic moiré grating is produced at $\sigma=0$

$$\overline{F}(x)\big|_{\sigma=0}=\frac{1}{2}+\frac{1}{2}\ \cos\left(\frac{2\pi}{\lambda}x\right) \tag{7}$$

and the time-averaged image is completely blurred out as $\sigma\to\infty$

$$\overline{F}(x)\big|_{\sigma\to\infty}=\frac{1}{2} \tag{8}$$

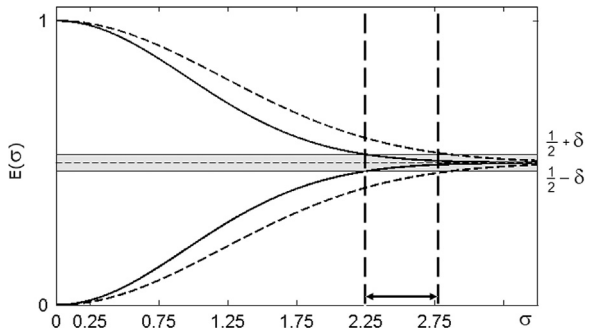

Fig. 1. The schematic diagram illustrating the experimental implementation of chaotic visual cryptography: the gray horizontal band illustrates the region where the time-averaged image is interpreted as a fully developed fringe; thin solid lines and thin dashed lines show the decay of the envelope function corresponding to pitches λ_0 and λ_1 accordingly; thick vertical dashed lines denote the region of σ which is applicable for chaotic visual cryptography.

3. Dynamic visual cryptography based on chaotic oscillations

The concept of dynamic visual cryptography is introduced in [8] and is based on the formation of time averaged moiré fringes in zones occupied by the secret image when the cover image is oscillated in a predefined law of motion (pitches of moiré gratings are slightly different for the secret and the background image). The law of motion $\xi(t)$ is now assumed to be a Gaussian process (since we consider chaotic oscillations). The decay of the modulating envelope function $\overline{E}(\sigma)$ at $\lambda_0=22\varepsilon=5.94$ mm and at $\lambda_1=20\varepsilon=5.4$ mm is illustrated in Fig. 1 by thin solid lines and thin dashed lines accordingly (ε is the size of the pixel and is equal to 0.27 mm). The horizontal dashed line is located at 0.5 and denotes the center of a time-averaged moiré fringe (time-averaged fringes become fully developed at $\sigma\to\infty$). A 2δ-width band around 0.5 is marked by a light gray color in Fig. 1; here δ stands for the blur level which is interpreted as a fully developed fringe by a human visual system [11]. In other words, the σ-region between two thick vertical lines (Fig. 1) is applicable for visual cryptography based on chaotic oscillations. The time averaged image of the moiré grating with λ_0-pitch will be interpreted as an interference fringe, and the moiré grating with λ_1-pitch will not be interpreted as an interference fringe in that range of σ.

In that respect the way how the secret image is leaked by chaotic dynamic visual cryptography is different from dynamic visual cryptography based on periodic oscillations [8]. Periodic oscillations can be used to leak the secret from the cover image in two different modes. Time-averaged fringes may form in the regions occupied by the secret image while a coarse time-averaged image is left in the background. Alternatively, time-averaged fringes may form in the background and a coarse time-averaged image is left in the regions occupied by the secret image – the formation of time-averaged fringes depends on the amplitude of harmonic oscillations. But chaotic dynamic cryptography does not allow such "flipping" of the time-averaged image. If the pitch of the moiré grating is higher for the secret than for the background image, then time-averaged fringes could form only in the background. If time-averaged fringes

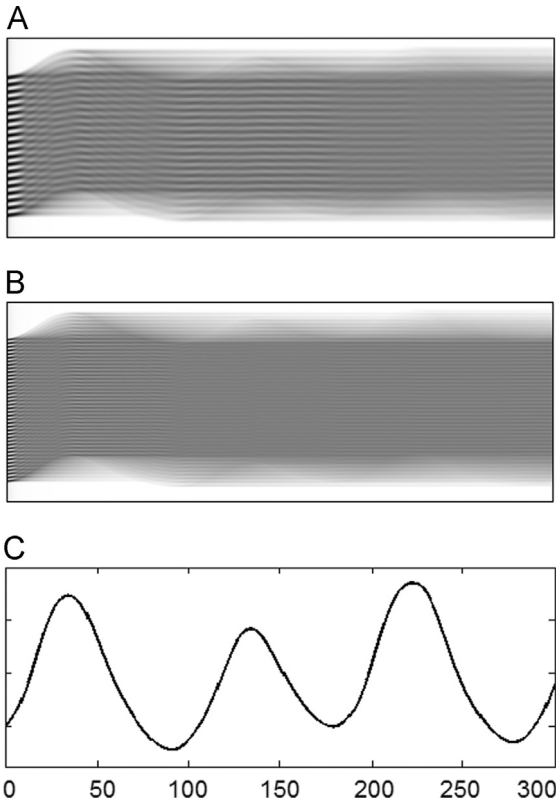

Fig. 2. Motion blur induced by chaotic oscillations for two different moiré gratings.

would form in the region occupied by the secret, they would also necessarily form in the background (Fig. 1) and visual decryption of the secret image would be impossible.

Note that the frequency of harmonic oscillations does not have any influence to the formation of time-averaged moiré fringes [16]. Nevertheless, this frequency must be high enough if the decoding is performed by a naked eye (the human visual system interprets a time-averaged fringe when the eye cannot follow the rapid oscillatory motion of the cover image) [8]. On the other hand, the exposure time must be long enough to accommodate a sufficient number of periods of harmonic oscillations if the time-averaged image is to be acquired by a photographic camera (analog or digital).

The situation is completely different when oscillations are chaotic. There are no longer any periods of oscillations. Time-averaged moiré fringes do not form at all when the cover image is blurred by a uni-directional chaotic law [15].

A computational illustration of the motion blur induced by chaotic oscillations is presented in Fig. 2. A paradigmatic nonlinear pendulum model with harmonic forcing [12] is exploited for the computational simulation of chaotic oscillations (Fig. 2C). Two moiré gratings with different pitches are used in parts A and B (Fig. 2); the exposure time varies from zero to 300 time steps along the x-axis. High contrast moiré gratings can be observed at the left parts of the time-averaged images. Both images (A and B) are eventually blurred out as the exposure time tends to infinity – but this process is different for different gratings (though the time history of nonlinear oscillations is identical).

Fig. 2 helps to reach two important observations. The first one is directly associated to the results presented in Fig. 1 – the motion blur induced by chaotic oscillations is different for different moiré gratings. The second one is important for the practical implementation of chaotic visual cryptography – finite exposure times are well applicable for these purposes too.

4. Computational experiments

The image encoding scheme used for the formation of the cover image for dynamic visual cryptography applications is based on stochastic initial phase deflection and boundary phase regularization algorithms [15]. A one-dimensional moiré grating with the pitch $\lambda_0 = 20\varepsilon = 5.4$ mm is used for the background and the moiré grating with the pitch equal to $\lambda_1 = 22\varepsilon = 5.94$ mm is used for the regions occupied by the secret image. Such encoding scheme allows hiding dichotomous pictures in the cover image. Note that the direction of deflections of the cover image from the state of equilibrium must be uni-directional and that direction must coincide with the longitudinal axis of the one-dimensional moiré grating.

The secret image is illustrated in Fig. 3A; the encoded cover image is shown in Fig. 3B. Note that a single cover image is used as a carrier of the secret visual information – the secret cannot be leaked from a static image (Fig. 3B). A number of computational experiments are performed by assuming that the cover image is oscillated according to the random time function $\xi(t)$ (the statistical standard σ is set to different values in parts C, D and E). The built-in random Gaussian number generator is used for building a discrete sequence of numbers with zero mean and standard equal to σ. Every random number defines the magnitude of deflection of the cover image from the state of equilibrium in the direction of moiré grating lines. The exposure time is set to 1000 discrete time moments – 1000 deflected copies of the cover image are used to construct time averaged images illustrated in Fig. 3 parts C, D and E. The secret image is almost un-interpretable in Fig. 3C – the standard $\sigma = 1.75$ is clearly too small (time-averaged fringes do not form neither in the background, nor in the region occupied by the secret image). This situation corresponds well to computational results presented in Fig. 1 – the values of the envelope function $\overline{E}(1.75)$ do not fit into the double δ width corridor at $\sigma = 1.75$. The secret image is leaked in Fig. 3D – time-averaged fringes are well developed in the background but are not fully developed at $\sigma = 2.5$. Note that the pitch of the moiré grating is higher in the areas occupied by the secret image than in the background ($\lambda_0 < \lambda_1$). But the rate of the decay of the envelope function $\overline{E}(\sigma)$ is inversely proportional to λ (Eq. (6)). The value $\sigma = 2.5$ fits into the zone applicable for chaotic visual cryptography (Fig. 1). A nearly-developed time-averaged moiré fringe can be observed in the background in Fig. 3D (while the time-averaged image in the zones occupied by the secret information is still coarse). Finally, the secret image is almost un-interpretable again at $\sigma = 3.25$ where time-averaged moiré fringes are fully developed both in the background and in the region occupied by the secret image.

The visually decoded secret image in Fig. 3D can be highlighted by using contrast enhancement techniques [17] – the resultant image is shown in Fig. 3F. Note that any contrast enhancements would not help to leak the secret from the encoded static cover image shown in Fig. 3B.

5. The experimental set-up

As mentioned previously, chaotic visual cryptography (as any visual cryptography scheme) requires special digital algorithms to encode the secret image – but the decoding process is a completely visual procedure which does not require a computer. The encoded cover image can be fixed onto the surface of a structure which performs chaotic oscillations.

The experimental setup for the implementation of this decoding technique does comprise two basic elements: a shaker table and an ordinary optical camera (Fig. 4). The encoded image is printed using an ordinary digital printer and is glued onto the

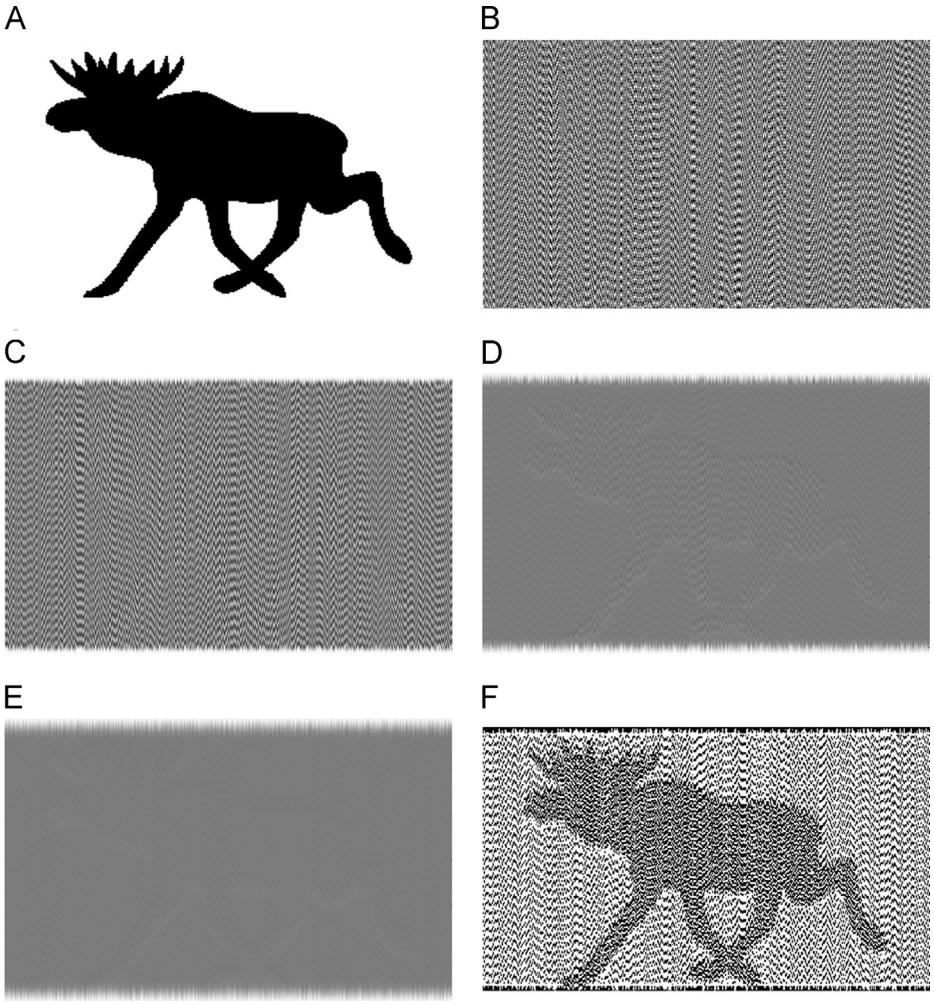

Fig. 3. Encoding and visual decryption of the secret image. The secret image is shown in A; the encoded cover image is shown in B; time-averaged cover images at $\sigma = 1.75$; $\sigma = 2.5$ and $\sigma = 3.25$ are illustrated in C, D and E respetively; the contrast enhanced image of D is shown in F.

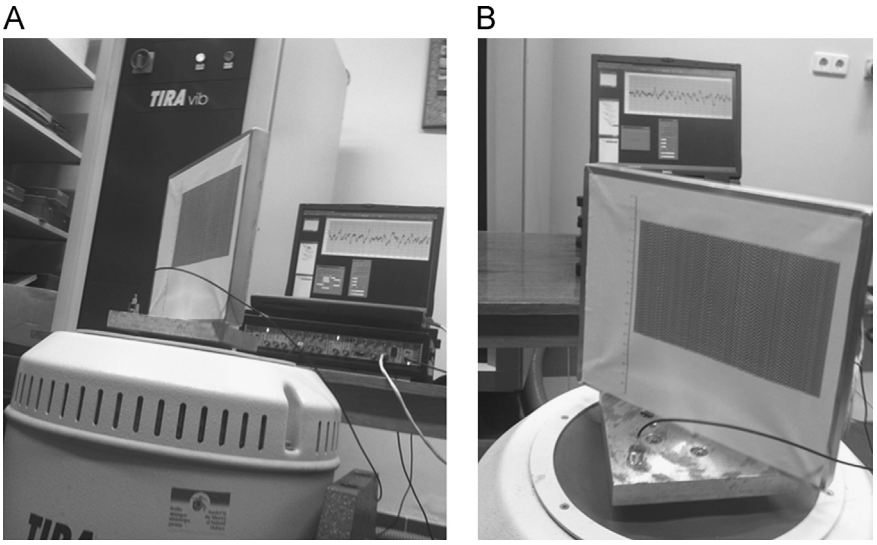

Fig. 4. The general view of the experimental setup is shown in part A; a lightweight piezoelectric accelerometer is used to monitor the vibration of the shaker table (part B).

surface of a rigid structure which is fixed to the head of the shaker table. It is important to check that this rigid fixture would not possess structural resonances at the pre-determined range of excitation frequencies – the visual decoding procedure is based on in-plane (not out-of-plane) oscillations [11].

The schematic diagram of the experimental setup is shown in Fig. 5. The shaker table TIRAvib 50300 is controlled by the amplifier TIRA BAA 2000-E. We use Esser-Audio filtered noise generator software to produce the white noise, pass it through the low pass filter (the range is set to 0–100 Hz) and feed the signal into the amplifier.

The embedded cover image and the Endevco 2225 lightweight piezoelectric accelerometer (sensitivity 0.07655 pC/m/s^2) is mounted on the head of the shaker table and connected to the Pulse Multi-analyzer system Type 3560 via charge to voltage converter Type 2647A (amplification 1 mV/pC); the whole process is controlled by Bruel & Kjaer Pulse LabShop. Thus, we do not only generate low frequency chaotic oscillations, but also control the instantaneous waveform of the generated motion of the shaker table. In other words, it is possible to set, monitor and control the parameters of chaotic oscillations.

6. Experimental results and discussion

The same encoded image (as shown in Fig. 3B) is glued to the vertical holder plate attached to the head of the shaker table (Fig. 4). The filtered noise generator is set to generate 30 s duration white noise signals in the loop mode and pass it through the low-pass filter (the peak frequency located at 30 Hz). The low-pass filter is used in order to mimic nonlinear chaotic oscillations of mechanical systems (it is clear that a shaker table would not be

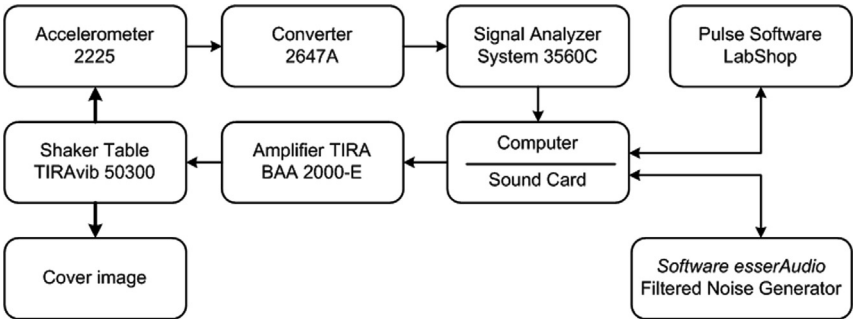

Fig. 5. The schematic diagram of the experimental setup.

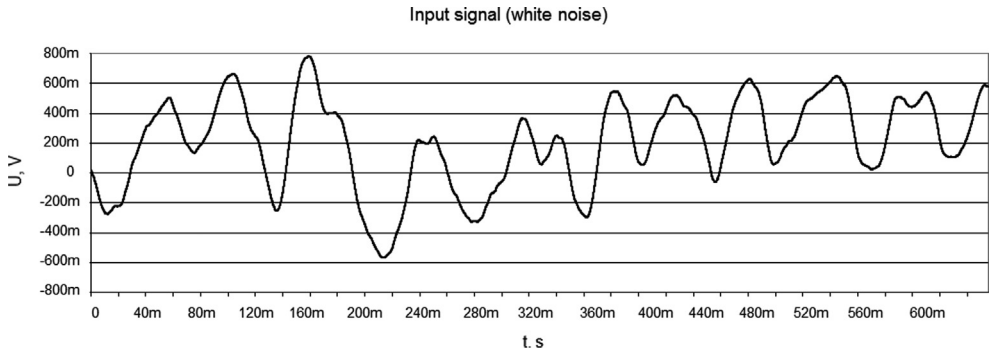

Fig. 6. The input signal from the white noise generator passed through the low-pass filter.

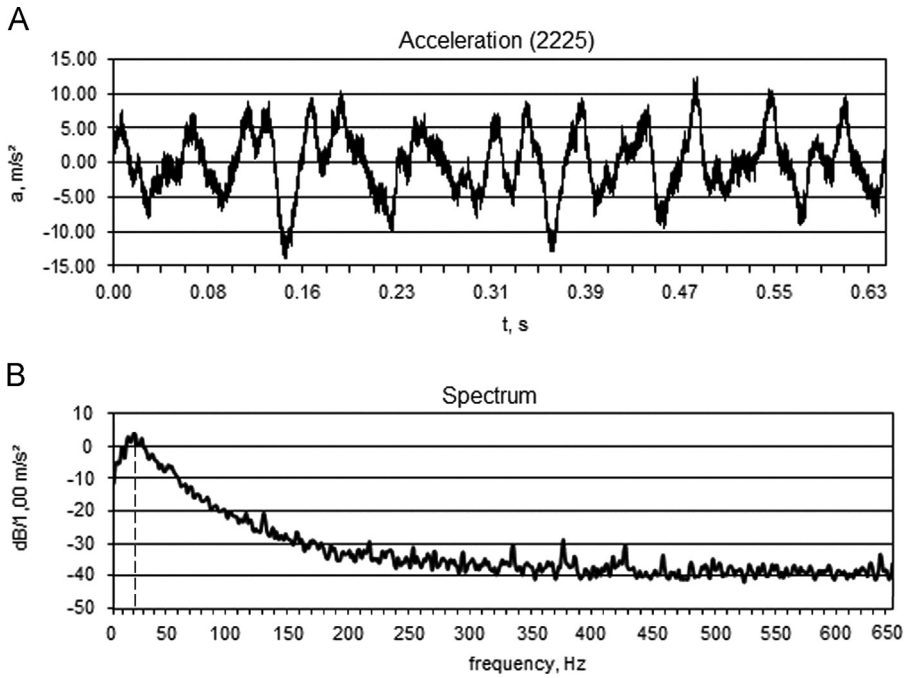

Fig. 7. The time plot from the piezoelectric accelerometer mounted on top of the shaker table (A) and the spectrum of the recorded signal (B); the maximum of the spectrum is denoted by a dashed line.

capable reproducing 10 kHz oscillations). The snapshot of the input signal to the TIRA amplifier is shown in Fig. 6.

The generated motion of the shaker table is registered by the piezoelectric accelerometer (Fig. 4); the time plot of the recorded signal is shown in Fig. 7A. Finally, the spectrum of the recorded signal is illustrated in Fig. 7B – it can be clearly seen that the maximum is reached at 22 Hz that almost corresponds to the peak frequency of the low-pass filter.

The applicability of dynamic visual cryptography for the control of periodic oscillations is investigated in [11]. Note that the frequency of harmonic oscillations does not have any influence to the formation of time-averaged moiré fringes – the exposure time just must be long enough to accommodate a sufficient number of periods of harmonic oscillations. It has been observed in [8,9] that 25–30 Hz is a sufficient frequency of harmonic oscillations to produce a well-interpretable secret image to a naked eye. That also explains the applicability of dynamic visual cryptography for chaotic oscillations. Chaotic visual cryptography would not be functional if the main peak of the spectrum of the chaotic signal would be located at, for example, 0.1 Hz – a naked eye would not be able to average slowly moving cover image. The time-averaged image does form when the eye cannot follow rapid oscillatory motion of the cover image.

The same holds for the digital camera. The exposure time should be long enough to accommodate a sufficient time interval representing the oscillatory motion of the cover image. The exposure time equal to 0.63 s (as shown in Fig. 7A) does represent a typical waveform of the reproduced chaotic motion and is sufficient to interpret the secret embedded image (Fig. 8). It can be noted that images interpreted by a naked eye are in general much better than recorded by the digital camera (due to comparatively short exposure times).

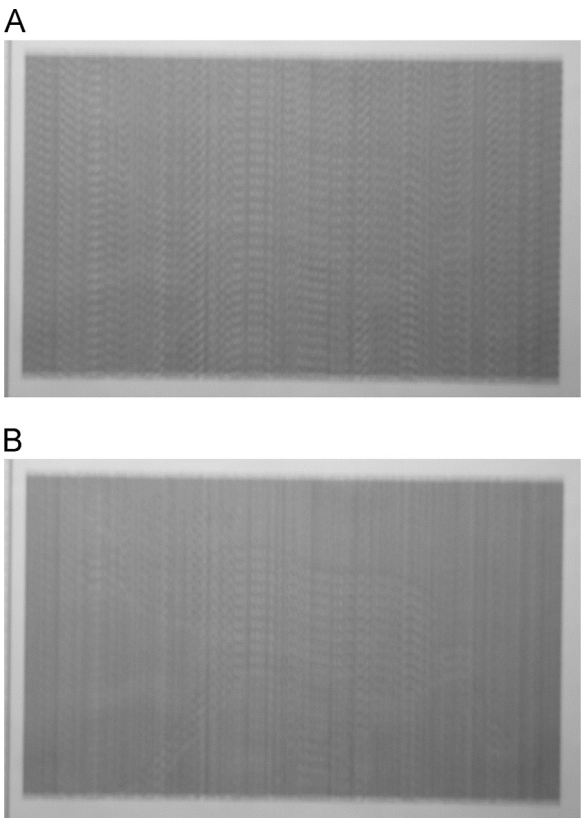

Fig. 8. Time averaged experimental images do reveal the secret image embedded into the cover image.

The parameters of the input signal are not changed during the experiment – the only parameter we did vary is the amplification of the control signal. The cover image remains static when the amplification is zero – then the secret image is not leaked from the cover image. The standard of the stochastic random variable representing chaotic oscillations increases as the amplification is enlarged. The secret image already can be interpreted in Fig. 8A – but time-averaged fringes are not developed neither in the zones occupied by the secret image, nor in the background. The secret image becomes clearer when the amplification is increased (Fig. 8B) – though time-averaged fringes are also not yet fully developed in the background.

7. Concluding remarks

Dynamic visual cryptography has been successfully used for optical control of vibration generation equipment. This whole-field non-destructive zero-energy method can be effectively exploited for optical assessment of different vibrating structures. The basic idea of this optical assessment technique is based on the fact that sophisticated computational tools are required to encode the secret image, but the decoding process is completely visual.

But it is well known that even a harmonic forcing of a nonlinear system may result in a complex chaotic response. And though the optical technique proposed in [11] does not depend on the frequency of periodic oscillations, it is not applicable for chaotic oscillations (the amplitude of oscillations cannot be preserved to be constant). This paper presents an important advancement which does allow applying dynamic visual cryptography for chaotic oscillations. Theoretical analysis does show that chaotic oscillations do not generate a pattern of time-averaged interference fringes – the time averaged image is continuously blurred as the intensity of chaotic oscillations is increased. But this rate of the contrast decay is sensitive to the pitch of the moiré grating in the static cover image. This optical effect allows the construction of a visual cryptography scheme which is able to leak the secret when the cover image is oscillated by a chaotic law. Moreover, the sizes of the pitches of moiré gratings used to encode the secret image can be preselected in such a way that the secret is leaked only at the predetermined intensity of chaotic oscillations. Different decay rates of the envelope function characterizing the formation of the time-averaged moiré fringes in the background and in the areas occupied by the secret image enable effective visual decoding of the embedded dichotomous image.

It is well known that motion induced blur can be used for the identification of the motion itself [18,19]. The proposed optical technique is not based on any de-blurring or trajectory reconstruction methods. Chaotic oscillations are assessed by direct optical interpretation of the time-averaged image.

Also, it is well known that optical techniques can be used to illustrate or even to simulate chaotic processes. A typical example is the famous optical demonstration of fractal geometry [20]. The proposed optical technique is completely different – no mirrors or composite images are used. But this optical technique still can be effectively used to assess chaotic processes by a naked eye. One can print a cover image on a sticker and glue it on a surface of a structure which must be monitored. The embedded secret image will be leaked only when this structure will perform predefined chaotic oscillations. Such engineering applications of the proposed optical technique are a definite topic of future research.

Acknowledgments

Financial support from the Lithuanian Science Council under project No. MIP-100/2012 is acknowledged.

References

[1] Naor M, Shamir A. Visual cryptography. Eurocrypt 1994:1–12.
[2] Young-Chang Hou. Visual cryptography for color images. Pattern Recognit 2003;36(7):1619–29.
[3] Cimato S, De Prisco R, De Santis A. Colored visual cryptography without color darkening. Theor Comput Sci 2007;374(1-3):261–76.
[4] Cimato S, De Santis A, Ferrara AL, Masucci B. Ideal contrast visual cryptography schemes with reversing. Inf Process Lett 2005;93(4):199–206.
[5] Ching-Nung Yang, Ting-Hao Chung. A general multi-secret visual cryptography scheme. Opt Commun 2010;283(24):4949–62.
[6] Ran-Zan Wang, Yung-Ching Lan, Yeuan-Kuen Lee, Shih-Yu Huang, Shyong-Jian Shyu, Tsorng-Lin Chia. Incrementing visual cryptography using random grids. Opt Commun 2010;283(21):4242–9.
[7] Yu-Chi Chen, Du-Shiau Tsai, Gwoboa Horng. A new authentication based cheating prevention scheme in Naor–Shamir's visual cryptography. J Visual Commun Image Represent 2012;23(8):1225–33.
[8] Ragulskis M, Aleksa A. Image hiding based on time-averaging moiré. Opt Commun 2009;282(14):2752–9.
[9] Ragulskis M, Aleksa A, Navickas Z. Image hiding based on time-averaged fringes produced by non-harmonic oscillations. J Opt A: Pure Appl Opt 2009;11(12):125411.
[10] Sakyte E, Palivonaite R, Aleksa A, Ragulskis M. Image hiding based on near-optimal moiré gratings. Opt Commun 2011;284(16–17):3954–64.
[11] Petrauskiene V, Aleksa A, Fedaravicius A, Ragulskis M. Dynamic visual cryptography for optical control of vibration generation equipment. Opt Lasers Eng 2012;50(6):869–76.
[12] Hilborn R. Chaos and Nonlinear Dynamics: An Introduction for Scientists and Engineers. Oxford: Oxford University Press; 1994.
[13] Petrov V, Qi Ouyang, Swinney HL. Resonant pattern formation in a chemical system. Nature 1997;388:655–7.
[14] Wolf A. Nonlinear dynamics: simplicity and universality in the transition to chaos. Nature 1983;305:182–3.
[15] Petrauskiene V, Palivonaite R, Aleksa A, Ragulskis M. Dynamic visual cryptography based on chaotic oscillations. Commun Nonlinear Sci Numer Simul 2013.
[16] KobayashiAS. Handbook on Experimental Mechanics. 2nd ed. Bethel, CT: SEM; 1993.
[17] Ragulskis M, Aleksa A, Maskeliunas R. Contrast enhancement of time-averaged fringes based on moving average mapping functions. Opt Lasers Eng 2009;47(7–8):768–73.
[18] Xu Ting-Fa, Zhao Peng. Object's translational speed measurement using motion blur information. Measurement 2012;43(9):1173–9.
[19] Deng Xiaoyu, Shen Yan, Song Mingli, Tao Dacheng, Bu Jiajun, Chen Chun. Video-based non-uniform object motion blur estimation and deblurring. Neurocomputing 2012;86:170–8.
[20] Sweet D, Ott E, Yorke JA. Complex topology in chaotic scattering. Nature 1999;399:315.